DOI: 10.1002/asia.200800354

New Wnt/β-Catenin Signaling Inhibitors Isolated from *Eleutherine palmifolia*

Xiaofan Li,[a] Takashi Ohtsuki,[a] Takashi Koyano,[b] Thaworn Kowithayakorn,[c] and Masami Ishibashi*[a]

Abstract: Aberrant Wnt/β-catenin signaling has recently been implicated in tumorigenesis. On the basis of our screening program targeting inhibition of TCF/β-catenin transcriptional activity, a plant extract of *Eleutherine palmifolia* was selected as a hit sample. Activity-guided fractionations led to the isolation of 15 naphthalene derivatives (**1**–**15**), including 4 new glucosides, eleutherinosides B–E (**1**–**4**), and 10 of the 15 compounds showed strong activities with high viability among 293T cells. Our data showed that **2** and **9** inhibited the transcription of TCF/β-catenin in SW480 colon cancer cells in a dose-dependent manner. These two compounds also showed selective cytotoxicity against three colorectal cancer cell lines. In addition, treatment with **9** led to a significant decrease in the level of nuclear β-catenin protein, suggesting this reduction to have resulted in the inhibitory effect of **9** on the transcription of TCF/β-catenin.

Keywords: biological activity · inhibitors · natural products · signal transduction · structure–activity relationships

Introduction

Wnt signaling is implicated in numerous aspects of development, cell biology, and physiology. Wnt/β-catenin signaling can also lead to the formation of tumors when aberrantly activated. Molecular studies have shown activating mutations of the Wnt signaling pathway as the cause of approximately 90% of colorectal cancers as well as other cancers, such as hepatocellular carcinoma and breast cancer.[1]

In the absence of Wnt ligands, β-catenin is phosphorylated by a destruction complex that contains the scaffolding proteins axin and adenomatous polyposis coli (Apc), and glycogen synthase kinase 3β (Gsk3β). Phosphorylated β-catenin is recognized by the E3 ubiquitin ligase β-TrCP and targeted for proteasomal degradation. Abnormal regulation of Wnt/β-catenin signaling and the subsequent up-regulation of β-catenin expression is a hallmark of the development of certain cancers. Excessive accumulation of cytosolic β-catenin leads to translocation to the nucleus, where this protein functions as a cofactor for transcription factors of T-cell factor/lymphoid enhancing factor (TCF/LEF) and leads to the stimulation of target genes including the c-myc and cyclin D1 genes. Thus, Wnt/β-catenin signaling is an attractive target for cancer therapy.[2] Given the low cost and biosafety of small-molecular compounds relative to biological drugs, there is significant interest in the search for Wnt/β-catenin signaling inhibitors among small-molecular natural products.

[a] X. Li, T. Ohtsuki, Prof. M. Ishibashi
Graduate School of Pharmaceutical Sciences, Chiba University
1-33 Yayoi-cho, Inage-ku, Chiba 263-8522 (Japan)
Fax: (+81) 43-290-2913
E-mail: mish@p.chiba-u.ac.jp

[b] Dr. T. Koyano
Temko Corporation
4-27-4 Honcho, Nakano, Tokyo 164-0012 (Japan)

[c] Prof. T. Kowithayakorn
Faculty of Agriculture, Khon Kaen University
Khon Kaen 40002 (Thailand)

Supporting information for this article is available on the WWW under http://dx.doi.org/10.1002/asia.200800354.

Results and Discussion

To investigate compounds inhibiting TCF/β-catenin transcription, screening of extracts from Thai plants was carried out. TCF/β-catenin transcriptional activity was measured using the cell line STF/293, which is a 293 cell line stably transfected with SuperTopflash (luciferase reporter plasmid containing 8 copies of the TCF/LEF binding site).[3] This plasmid is widely used to evaluate β-catenin-dependent signaling events that drive the expression of TCF. STF/293 cells have low TCF/β-catenin transcriptional activity because

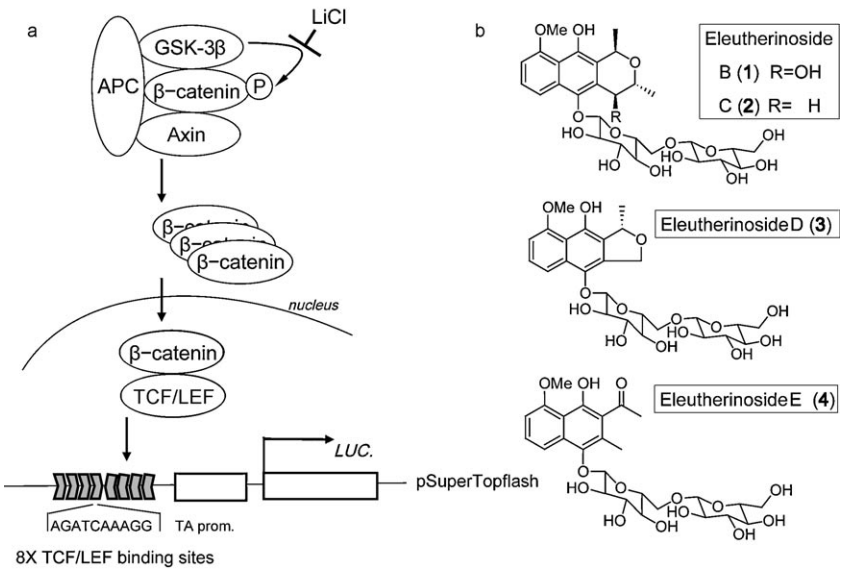

Figure 1. a) The assay system using the STF/293 cell line, which was a 293 cell line stably transfected with SuperTopflash plasmid; b) structure of eleutherinosides B–E.

of the low endogenous levels of β-catenin protein. However, Wnt signaling in the cells can be stimulated by inhibiting GSK-3β. LiCl, an inhibitor of GSK-3β, causes the accumulation of non-phosphorylated β-catenin and, as a result, an increase in TCF/β-catenin transcription.[4,5] Therefore, the STF/293 reporter cells combined with LiCl treatment were used to evaluate SuperTopflash activity (Figure 1a). The extracts inhibiting SuperTopflash activity were further investigated for SuperFopflash activity (luciferase reporter plasmid containing 8 copies of a mutant TCF/LEF binding site) to exclude nonselective inhibitors of Wnt signaling. As a result, we found that *Eleutherine palmifolia* (Iridaceae) selectively suppressed TCF/β-catenin transcriptional activity (45% inhibition at 5 μg mL^{-1}) and its active constituents were further studied as follows.

The MeOH extract of *E. palmifolia* bulbs was partitioned successively with EtOAc, *n*BuOH, and water. The active *n*BuOH layer (65% inhibition at 5 μg mL^{-1}) was then separated by silica gel column chromatography, followed by ODS-HPLC to yield four new compounds, eleutherinoside B (**1**), C (**2**), D (**3**), and E (**4**) (Figure 1b), as well as three known compounds, **5**,[6a] **6**, and **7**.[6b] The active EtOAc layer (91% inhibition at 5 μg mL^{-1}) was subjected to silica gel column chromatography, followed by ODS-HPLC to yield eight known compounds **8**–**15**.[7–11]

Eleutherinoside C (**2**) was obtained as a reddish-brown powder. The HRFAB-MS spectrum suggested a molecular formula of $C_{28}H_{38}O_{14}$. The ^{13}C NMR, DEPT, and HMQC spectra showed signals of 10 aromatic carbon atoms, 2 secondary methyl carbon atoms, 1 methoxy carbon atom, 1 methylene carbon atom, and 2 glucosyl residues (Table 1). The ^{1}H NMR spectrum showed signals of two secondary methyl groups ($\delta=1.21$ ppm, 3H, d, $J=6.0$ Hz; $\delta=1.50$ ppm, 3H, d, $J=6.5$ Hz), one methoxy group ($\delta=4.00$ ppm, s), two methine protons ($\delta=4.10$ ppm, m; $\delta=5.06$ ppm, q, $J=6.3$ Hz) attached to an oxygen function, one pair of methylene protons ($\delta=2.26$ ppm, dd, $J=17.0$, 5.5 Hz; $\delta=3.55$, dd, $J=17.0$, 2.8 Hz), three aromatic protons ($\delta=8.09$ ppm, d, $J=8.5$ Hz, H-6; $\delta=7.28$ ppm, dd, $J=8.5$, 8.0 Hz, H-7; $\delta=6.88$ ppm, d, $J=8.0$ Hz, H-8), and two anomeric protons ($\delta=4.61$ ppm, d, $J=7.5$ Hz, 1′-H; $\delta=4.03$ ppm, d, $J=8.0$ Hz, H-1″). Furthermore, the HMBC and COSY spectra indicated the presence of a tri-substituted benzene ring with three consecutive protons, as shown in Figure 2. The partial structure of the dihydropyran was established on the basis of HMBC correlations between $\delta=5.06$ (H-1) and 62.0 (C-3) and 128.4 ppm (C-12), as well as a correlation between $\delta=2.26$ (H-4) and 120.6 ppm (C-11). The COSY correlations between $\delta=1.21$ (1-Me) and 5.06 ppm (H-1), as well as $\delta=1.50$ (3-Me) and 4.10 ppm (H-3) indicated two methyl groups attached to C-1 and C-3. The HMBC correlations between $\delta=8.09$ (H-6) and 2.26 (H-4) and 141.0 ppm (C-5), as well as between $\delta=5.06$ (H-1) and 145.4 ppm (C-10), indicated that the benzene ring and the dihydropyran ring were linked by another benezene ring, which together made up a naphthopyran skeleton. This skeleton together with two sugar rings accounted for the 10 unsaturated equivalents. Moreover, the correlations between $\delta=4.00$ (-OMe) and 56.3 (C-9), 4.61 (H-1′), and 141.0 ppm (C-5), and $\delta=4.03$ (H-1″) and 68.4 ppm (C-6′) indicated that the methoxy group, and the two glucose units were connected as shown in Figure 2. Hydrolysis of eleutherinoside C (**2**) with naringinase afforded D-glucose, which was identified by HPLC with an authentic sample after its conversion

Abstract in Japanese:

Wnt シグナルの異常な活性化は，種々のがんの発生原因になっていることが知られている。本研究では本経路を阻害する天然物の発見を目指して，熱帯植物を対象にスクリーニングを行った。活性が認められた *Eleutherine palmifolia*（アヤメ科）より新規 4 種を含む 15 種のナフタレン化合物を単離し、その内 10 種は比較的強い TCF/β-catenin 転写阻害活性を示した。また化合物 **2** と **9** は大腸がん細胞 SW480 においても転写阻害活性が認められ、大腸がん細胞株 3 種に対し選択的な細胞毒性を示した。また化合物 **9** の処理により、SW480 細胞の核内の β-catenin 量の減少が認められ、この減少が Wnt シグナル阻害のメカニズムと示唆された。

Table 1. ^{1}H and ^{13}C NMR data of Eleutherinosides B–E.

	Eleutherinoside B ([D$_6$]DMSO)		Eleutherinoside C ([D$_6$]DMSO)			Eleutherinoside D ([D$_6$]DMSO)			Eleutherinoside E (CD_3OD)	
position	δ_H [ppm] (J [Hz])	δ_C [ppm]	δ_H [ppm] (J [Hz])	δ_C [ppm]	position	δ_H [ppm] (J [Hz])	δ_C [ppm]	position	δ_H [ppm] (J [Hz])	δ_C [ppm]
1	5.01 q (6.5)	64.9	5.06 q (6.5)	67.5	1	5.35 qd (6.3, 1.0)	78.3	1		143.8
3	4.05 overlap	69.3	4.10 m	62.0	3	5.42 dd (13.4, 1.0)	70.6	2		127.2
4	4.68 brt (3.3)	64.0	2.26 dd (17.0, 5.5)	31.2		5.05 d (13.4)		3		125.8
			3.55 dd (17.0, 2.8)		4		137.6	4		149.6
5		142.3		141.0	5	8.04 d (8.5)	115.7	5		158.0
6	8.25 d (8.5)	116.2	8.09 d (8.5)	115.6	6	7.33 dd (8.5, 8.0)	125.7	6	6.95 d (8.0)	105.9
7	7.35 dd (8.5, 8.0)	125.8	7.28 dd (8.5, 8.0)	125.4	7	6.94 d (8.0)	104.5	7	7.39 dd (8.0, 8.5)	128.2
8	6.98 d (8.0)	105.2	6.88 d (8.0)	104.0	8		156.2	8	8.03 d (8.5)	117.8
9		155.7		155.8	9		143.7	9		132.6
10		145.8		145.4	10		124.7	10		114.9
11		119.9		120.6	11		130.8	11		208.4
12		128.8		128.4	12		130.3	11-Me	2.60 s	32.6
13		127.4		127.3	13		114.9	2-Me	2.32 s	14.4
14		114.2		112.9	1-Me	1.47 d (8.5)	20.1	5-OMe	4.08 s	56.9
1-Me	1.55 d (6.2)	21.8	1.50 d (6.5)	19.1	8-OMe	4.01 s	56.2			
3-Me	1.02 d (6.5)	17.9	1.21 d (6.0)	22.2						
9-OMe	4.05 s	56.4	4.00 s	56.3						
1′	4.77 d (8.0)	103.7	4.61 d (7.5)	104.5	1′	4.54 d (7.5)	104.6	1′	4.72 d (8.0)	104.4
2′	2.85 ddd (8.0,8.0,3.0)	73.6	3.43 m	74.2	2′	3.36 overlap	73.8	2′	3.62 m	75.9
3′	3.07 m	76.1	3.15 m	75.2	3′	3.19 m	76.6	3′	3.42 m	77.7
4′	2.98 m	69.7	3.22 m	69.7	4′	3.19 m	69.9	4′	3.42 m	71.5
5′	3.03 m	76.8	3.22 m	76.3	5′	3.33 overlap	75.2	5′	3.26 m	77.5
6′	4.05 overlap	68.8	3.47 dd (11.0, 5.5)	68.4	6′	3.58 dd (11.0, 6.0)	68.7	6′	3.69 dd (12.0, 6.0)	69.8
	3.50 dd (9.5, 9.0)		3.93 brd (11.0)			3.97 brd (11.0)			3.99 dd (12.0, 2.0)	
1″	4.05 d (8.0)	102.7	4.03 d (8.0)	103.0	1″	4.13 d (7.5)	103.1	1″	4.07 d (9.0)	106.0
2″	3.43 m	73.7	2.89 brt (8.0)	73.6	2″	2.95 ddd (8.5, 5.0)	73.5	2″	3.04 dd (8.0, 9.0)	75.1
3″	3.36 overlap	75.9	3.06 dd (8.0, 8.5)	76.8	3″	3.09 m	76.8	3″	3.13 t (9.0)	77.9
4″	3.15 m	70.5	3.00 m	70.2	4″	3.03 m	70.6	4″	3.20 t (9.3)	71.7
5″	3.38 m	75.3	2.98 m	76.9	5″	3.03 m	78.3	5″	3.01 ddd (9.3, 6.0, 2.0)	77.9
6″	3,62 dd (10.0, 5.0)	60.9	3.64 brd (11.5)	61.2	6″	3.63 dd (11.5, 5.5)	61.0	6″	3.59 m	62.7
	3.36 overlap		3.40 overlap			3.39 dd (11.5, 4.5)			3.79 dd (12.0, 2.0)	

into a thiazolidine derivative. The hydrolysis also afforded isoeleutherin (**9**), which was identified by a comparison of NMR and $[\alpha]_D$ data with literature data.[8]

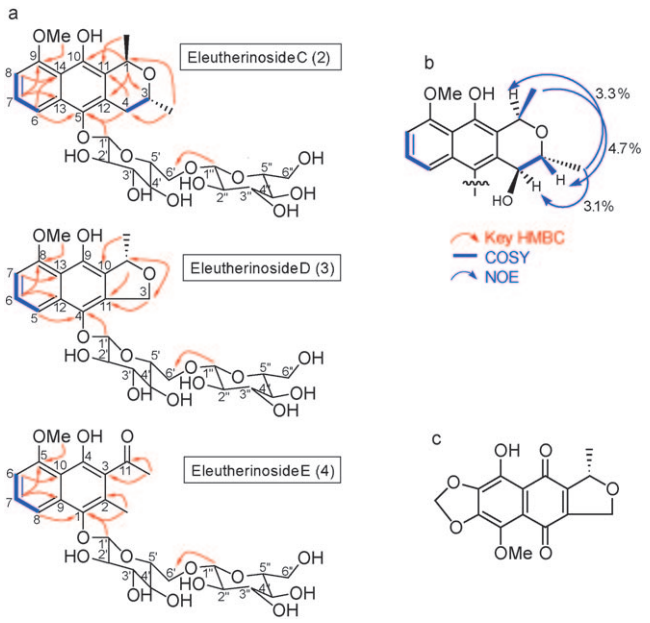

Figure 2. a) Key ^{1}H–^{1}H COSY and HMBC data for eleutherinosides B–E; b) NOE effect of eleutherinoside B; c) structure of ventilong C.

Eleutherinoside B (**1**), with the molecular formula $C_{28}H_{38}O_{15}$, showed a similar signal pattern to eleutherinoside C (**2**) in the ^{1}H- and ^{13}C NMR spectra, except that the methylene protons (4-CH_2) in **2** were replaced by a hydroxy group and a methine proton ($\delta = 4.68$ ppm, brt, $J = 3.3$ Hz) in **1**. Since **1** has one more oxygen atom than **2**, the structure of eleutherinoside B (**1**) was revealed, as shown in Figure 2, which was consistent with the COSY and HMBC correlations observed for **1**. Furthermore, the configuration of C-1 and C-3 of the aglycone of **1** was found to be in parallel based on the NOE experiments (Figure 2b). Hydrolysis of **1** with naringinase afforded D-glucose, which was identified by comparison of the HPLC data with that of an authentic sample after its conversion into a thiazolidine derivative.[12]

Eleutherinoside D (**3**), with the molecular formula $C_{26}H_{34}O_{14}$, showed signals of one secondary methyl ($\delta =$ 1.47 ppm, 3H, d, $J = 8.5$ Hz), one methoxy ($\delta = 4.01$ ppm, 3H, s), one methine proton ($\delta = 5.35$ ppm, qd, $J = 6.3$, 1.0 Hz) attached to an oxygen function, one pair of methylene protons ($\delta = 5.05$ ppm, d, $J = 13.4$ Hz; $\delta = 5.42$ ppm, dd, $J = 13.4$, 1.0 Hz), three aromatic protons ($\delta = 8.04$ ppm, d, $J = 8.5$ Hz, H-5; $\delta = 7.33$ ppm, dd, $J = 8.5$, 8.0 Hz, H-6; $\delta =$ 6.94 ppm, d, $J = 8.0$ Hz, H-7), and two anomeric protons

($\delta = 4.54$ ppm, d, $J = 7.5$ Hz, H-1′; $\delta = 4.13$ ppm, d, $J = 7.5$ Hz, H-1″) from two glucose units in its ^{1}H NMR spectrum. Furthermore, the COSY and HMBC spectra suggested the presence of a naphthalene moiety similar to that of **2**. The HMBC correlations between $\delta = 5.35$ (H-1) and 70.6 ppm (C-3); $\delta = 5.42$ (H-3) and 78.3 ppm (C-1); H-1 and H-3 and $\delta = 130.8$ (C-11) as well as 1.47 ppm (1-Me) and 124.7 ppm (C-10) indicated a methyl-substituted furan unit connected to the naphthalene moiety. The HMBC correlation between $\delta = 4.54$ (H-1′) and 137.6 ppm (C-4) and between $\delta = 4.13$ (H-1″) and 68.7 ppm (C-6′) indicated that the two glucose units were connected as shown in Figure 2. Hydrolysis of **3** with naringinase afforded D-glucose, which was identified by comparison of the HPLC data with that of an authentic sample after its conversion into a thiazolidine derivative. The hydrolysis also afforded eleutherinone (**12**), which was identified by comparison of the NMR and $[\alpha]_D$ data with literature data.[11] However, the absolute configuration of **12** had not been determined in the literature.[11] By comparison of the CD data of the aglycon from **3** with that of a known compound, ventilong C (structure shown in Figure 2c),[13] eleutherinoside D (**3**) was assigned an *S* configuration at C-1 since the CD data showed the same Cotton effects and the two compounds showed similar optical rotations (see the Experimental Section).

Eleutherinoside E (**4**), with the molecular formula $C_{26}H_{34}O_{14}$, showed signals arising from two methyl groups ($\delta = 2.60$ ppm, 3H, s; 2.32, 3H, s), one methoxy group ($\delta =$ 4.08 ppm, 3H, s), three aromatic protons ($\delta = 6.95$ ppm, d, $J = 8.0$ Hz, 6-H; $\delta = 7.39$ ppm, dd, $J = 8.5$, 8.0 Hz, H-7; $\delta =$ 8.03 ppm, d, $J = 8.5$ Hz, H-8), and two anomeric protons ($\delta = 4.72$ ppm, d, $J = 8.0$ Hz, H-1′; $\delta = 4.07$ ppm, d, $J = 9.0$ Hz, H-1") from two glucose units in its ^{1}H NMR spectrum. Furthermore, the COSY and HMBC spectra suggested a naphthalene moiety similar to that of **2**. The HMBC correlations between $\delta = 2.60$ (11-Me) and 208.4 (C-11) and 125.8 ppm (C-3), and between $\delta = 2.32$ (2-Me) and 143.8 (C-1) and 127.2 ppm (C-2), indicated an acetyl and a methyl group connected to the naphthalene moiety at C-3 and C-2, respectively. The correlations from $\delta = 4.72$ (H-1′) to 143.8 ppm (C-1) and $\delta = 4.07$ (H-1″) to 69.8 ppm (C-6′) indicated that the two glucose units were connected as shown in Figure 2. Hydrolysis of **4** with naringinase afforded D-glucose, which was identified by comparison of the HPLC data with that of an authentic sample after its conversion into a thiazolidine derivative.

Along with the 4 new compounds, 11 known compounds were also obtained. They were identified as eleutherinoside A (**5**),[6a] eleuthoside B (**6**),[6b] eleuthoside C (**7**),[6b] 2-acetyl-8-methyl naphthalene-1, 4-dione (**8**),[7] isoeleutherine (**9**),[8] dihydroeleutherinol (**10**),[9] 4-hydroxy-isoeleutherine (**11**),[10] eleutherinone (**12**),[11] eleutherol (**13**),[8] eleutherine (**14**),[8] and hongconin (**15**)[8] by comparison of the NMR and $[\alpha]_D$ data with literature data.

All compounds were tested for TCF/β-catenin transcriptional activity by using STF/293 cells. Cytotoxicity against 293T cells as well as SuperFopflash activity was also tested. Except for **4**, **6**, **8**, **13**, and **15**, all of the compounds inhibited TCF/β-catenin transcriptional activity in a dose-dependent manner with high cell viability and a small decrease in SuperFopflash activity. The results are shown in Table 2, along with those for quercetin, a previously reported small molecular TCF/β-catenin signaling inhibitor,[14] as a positive control. According to Table 2, the naphthalene glucosides (**2**, **7**, and **1**) showed more activity than their naphthoquinone aglycons (**9**, **14**, and **11**). Moreover, **4** did not inhibit SuperTopflash activity, whereas **8** inhibited both SuperTopflash and SuperFopflash activity. Therefore, loss of the pyran ring resulted in a loss of inhibitory activity against TCF/β-catenin transcription. The presence of a pyran ring, or furan ring, such as in **3** and **12**, was indispensable for the activities.

To investigate the effect of these compounds in human colorectal cancer cells, cytotoxicity against DLD1, HCT116, and SW480 cells was tested using **2** and **9**, which were isolated in abundance. As shown in Figure 3, both **2** and **9** exhibited selective cytotoxicity against the three colorectal cancer cell lines compared with human embryonic kidney cells (293T). Furthermore, the TCF/β-catenin transcriptional activity in SW480 cells was examined to show that these compounds inhibited Wnt/β-catenin signaling in SW480 cells dose-dependently. The results indicated the selective cytotoxicity of **2** and **9** against colorectal cancer cells to be mediated by their ability to down-regulate Wnt/β-catenin signaling.

To investigate the effect of **9** on Wnt/β-catenin signaling-related factors, the protein levels of TCF, β-catenin, and a Wnt signaling target, c-myc, were examined with a Western blot analysis (Figure 4). SW480 cells were incubated on 60 mm dishes with **9** for 24 h and cellular lysates were isolated. The protein level of TCF was unchanged, whereas there was a moderate decrease in β-catenin. A decrease in c-myc was also detected on treatment with **9** at 10 $\mu g\,mL^{-1}$. Translocation of β-catenin into the nucleus was required for its transcriptional activity as a coactivator. Because β-catenin exists both in the cytosol and in the nucleus, cytosolic and nuclear lysates from **9**-treated SW480 cells were isolated, and the protein levels of β-catenin in both lysates were explored. As shown in Figure 4, a significant decrease in nuclear β-catenin was found on treatment with **9** at 10 $\mu g\,mL^{-1}$, whereas the protein level of cytosolic β-catenin was unchanged. All of these results indicated that the suppression of nuclear β-catenin was one of the reasons for the inhibitory effect of **9** on the transcription of TCF/β-catenin.

Conclusions

Some herbal plants from *Eleutherine* species have been used as a vermifuge, for painful and irregular menstruation,[15] for intestinal disorders,[16,17] and as an abortive and antifertility agent.[18] The bulbs of this plant have also been used to treat intestinal infections, and the rhizome was reported as a folk medicine for the treatment of coronary disorders.[19] Some compounds present in the genus display important biological

Table 2. Selective inhibition of TCF/β-catenin transcription and structure–activity correlation of the isolated naphthalene compounds.

	Structure	Compound No.	IC50 [μM][a]	SuperFopflash [%][b]	Viability [%][b]
glucosides (active)	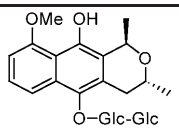	**2**	2.1	100%	96%
	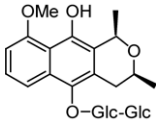	**7**	3.1	100%	94%
	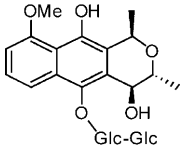	**1**	2.5	100%	94%
	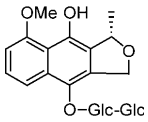	**3**	2.6	100%	100%
	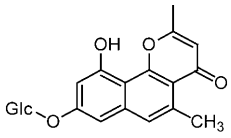	**5**	10.8	100%	100%
	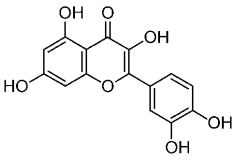 quercetin[c]		30.4	72%	98%

	Structure	Compound No.	IC_{50} [μM][a]	SuperFopflash [%][b]	Viability [%][b]
aglycones (active)	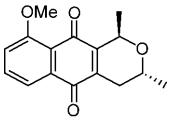	**9**	9.5	87%	100%
	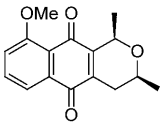	**14**	12.9	88%	100%
	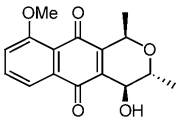	**11**	6.5	69%	88%
	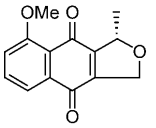	**12**	3.5	82%	100%
	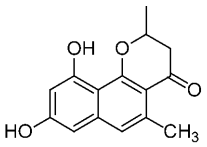	**10**	13.5	79%	100%

activity. Eleutherin (**14**) was described to form a type of noncleavable complex with topoisomerase II with stereospecific and selective inhibitory activity.[20] Inhibitory activity of isoeleutherin (**9**) and isoeleutherol against HIV replication in H9 lymphocytes[20] was also reported. Herein, we found this plant to have inhibitory effects on the transcription of TCF/β-catenin upon screening over 200 tropical plants. Activity-guided separation led to 15 naphthalene compounds, including five new ones. Ten compounds showed strong activities in a dose-dependent manner with high cell viability and a small decrease in SuperFopflash activity. We found that the naphthalene glucosides (**2**, **7**, and **1**) showed more activity than the naphthoquinone aglycons (**9**, **14**, and **11**). Moreover, the presence of a pyran ring or furan ring was indispensable for the activities. Interestingly, naphthalene compounds possessing a pyranone or furanone ring, such as **6**, **13**, and **15**, showed no activity. It was also reported that the naphthopyrans (isoeletherin **9** and eleutherin **14**) and naphthofuran (eleutherinone **12**) showed strong antifungal activity, whereas the naphthopyranone (eleutherol **13**) was inactive.[11]

As the importance of Wnt/β-catenin signaling in relation to tumorigenesis has become evident, many more studies[24,25] on TCF/β-catenin inhibitors and their inhibitory mechanism are being conducted. Our data shows that compounds **2** and **9** inhibited the transcription of TCF/β-catenin in SW480 colon cancer cells in a dose-dependent manner. The two compounds also showed selective cytotoxicity against three colorectal cancer cell lines compared with human

	Structure	Compound No.	IC_{50} [μM][a]	SuperFopflash [%][b]	Viability [%][b]
other naphthalenes (inactive)	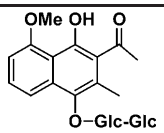	**4**	>20	100%	100%
	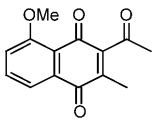	**8**	10.3	24%	79%
	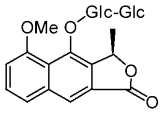	**6**	>20	100%	100%
	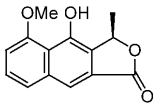	**13**	>40	n.d.	100%
	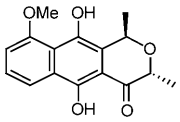	**15**	>40	n.d.	100%

[a] The concentration of compound that inhibits 50% of TCF/β-catenin transcription activity; [b] SuperFOPflash activity and viability of the cells on treatment with the compounds at the concentration of IC_{50}. n.d.: not determined; [c] quercetin,[14] positive control.

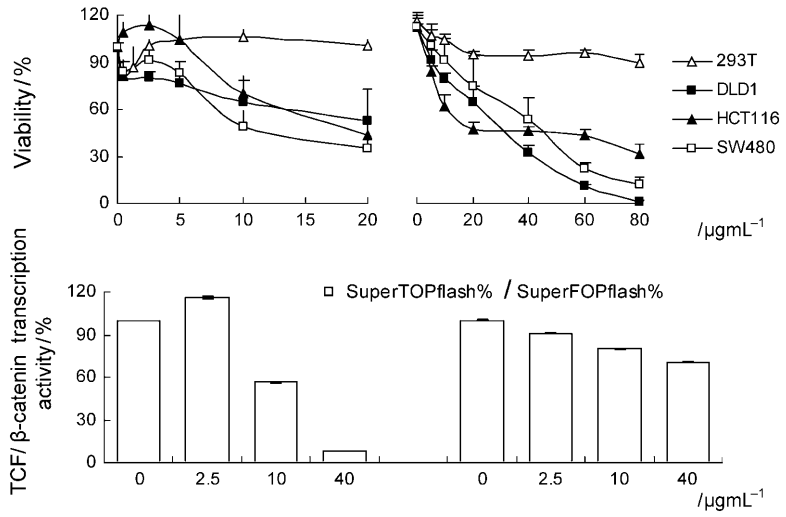

Figure 3. Cytotoxicity (top) and inhibition of TCF/β-catenin transcription (bottom; defined as the value of SuperTopflash activity divided by the SuperFopflash activity) induced by **9** (left) and **2** (right).

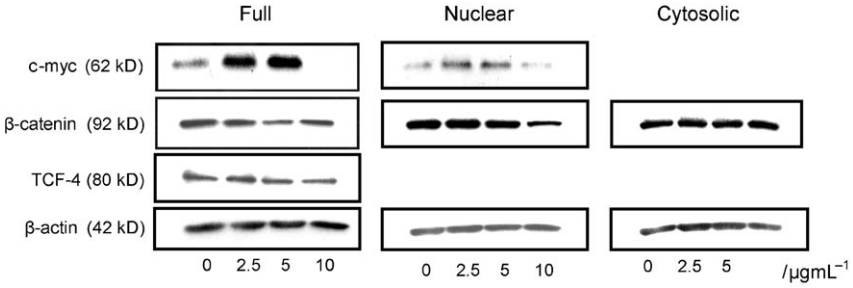

Figure 4. Western blot analysis of the effects of **9** in SW480 cells.

embryonic kidney cells (293T). These results indicate the selective cytotoxicity of **2** and **9** against colorectal cancer cells to be mediated by an ability to downregulate Wnt/β-catenin signaling. The effect of the inhibitors on the Wnt signaling target gene was important for the function of the cells. We found that compound **9** downregulated c-myc expression at the protein level at a concentration of 10 $\mu g\,mL^{-1}$. It was not clear why **9** showed upregulation of c-myc expression at lower concentrations of 2.5 and 5 $\mu g\,mL^{-1}$. It has been reported that both a decrease and an increase in c-myc leads to apoptosis;[21] thus, we concluded that the up-regulation of c-myc expression by **9** at low concentrations did not counteract its cytotoxic effect in colon cancer cells. Next, our data showed that treatment with **9** led to a significant decrease in the protein level of nuclear β-catenin. β-catenin is ubiquitous and moves freely in the cell. It contributes to cell–cell adhesion in the membrane and functions as a transcriptional activator in the nucleus. Here, we could conclude that this reduction in nuclear β-catenin resulted in the inhibitory effect of **9** on TCF/β-catenin transcription. Finally, it should be noted that this is the first report of a series of naphthalene compounds with inhibitory activity against Wnt signaling obtained from natural sources. Because of the low cost and biosafety,[22] further studies and usage of the active compounds can be expected.

Experimental Section

Plant material: Plant materials of *Eleutherine palmifolia* were collected from Khon Kaen, Thailand. Voucher

specimens (6–484) were deposited in our laboratory.

Cell cultures: HCT116 and DLD1 cells were purchased from ATCC; SW480 cells were derived from the Institute of Development, Aging, and Cancer, Tohoku University; STF/293 cells were a generous gift from Prof. Jeremy Nathans (Johns Hopkins Medical School). STF/293, 293T, SW480, and HCT116 cells were cultured in Dulbecco's modified eagle medium (Wako) with 10% FBS. DLD1 cells were cultured in RPMI-1640 medium (Wako) with 10% FBS. Cultures were maintained in a humidified incubator at 37°C in 5% CO_2/95% air.

Transfection and luciferase assay: Transient transfection was performed using Lipofectamine 2000 (Invitrogen, USA). Briefly, 1×10^5 cells (293T or SW480) were split into 24-well plates. After 24 h, cells were transfected with 1 μg of the luciferase reporter constructs (SuperTopflash or SuperFopflash, a generous gift from Prof. Randall T. Moon, University of Washington) and 0.05 μg of pRL-CMV plasmid (Promega, USA) for normalization. At 3 h posttransfection, compounds were added with a medium containing FBS. Of note, 293T cells were treated with compounds in a FBS-containing medium combined with 15 mM of LiCl. Cells incubated for 24 h were lysed in Passive lysis buffer (Promega, 50 μL well^{-1}) and luciferase activity was measured with a Dual-Glo Luciferase Assay System (Promega). For stable reporter cells, STF/293 cells (3×10^4) were split into 96-well plates and 24 h later treated with compounds combined with 15 mM LiCl. After incubation for 24 h, cells were lysed with CCLR (cell culture lysis reagent; 20 μL well^{-1}, Promega) and luciferase activity was measured with a Luciferase Assay System (Promega). Assays were performed at least in triplicate.

Assay of cell viability (FMCA assay):[23] SW480, HCT116, DLD1, and 293T cells (6×10^3) were split into 96-well plates and incubated for 24 h. Cells were treated with compounds and incubated for 24 h. They were treated with fluorescein diacetate (Wako) in PBS buffer (10 μg mL^{-1}), and after 1 h of incubation, fluorescence was detected. Assays were performed at least in triplicate.

Activity-guided extraction and isolation: The MeOH extract (10.3 g) of bulbs of *E. palmifolia* was dissolved in 10% aqueous MeOH, and partitioned successively with EtOAc (100 mL×2) and *n*BuOH (100 mL×2) to give three layers (EtOAc layer, 2.5 g, 91% inhibition of TCF/β-catenin transcription; *n*BuOH layer, 3.9 g, 65% inhibition; water layer, 56% inhibition at 5 μg mL^{-1}, respectively). The BuOH layer was then separated by chromatography on a silica gel PSQ100B column ($\phi=28\times500$ mm) to give fraction 1a (72 mg, eluted with 1100 mL of $CHCl_3$/MeOH 9:1, 4.3% inhibition at 2.5 μg mL^{-1}), 1b (215 mg, eluted with 1100 mL of $CHCl_3$/MeOH 8.5:1.5, 5.9% inhibition at 2.5 μg mL^{-1}), 1c (177 mg, eluted with 400 mL of $CHCl_3$/MeOH 8:2, 67% inhibition at 2.5 μg mL^{-1}), 1d (842 mg, eluted with 600 mL of $CHCl_3$/MeOH 8:2, 64% inhibition at 2.5 μg mL^{-1}), and 1e (2.3 g, eluted with 4300 mL of MeOH, 12% inhibition at 2.5 μg mL^{-1}). Fraction 1c was suspended in $CHCl_3$ and the precipitate was collected to give eleutherinoside A (**5**, 40 mg). Fraction 1d was purified by ODS-HPLC (Mightysil RP18 column, $\phi=10\times250$ mm; eluted with 47% aqueous MeOH; flow rate, 2 mL min^{-1}) to give eleutherinoside E (**4**, 2.5 mg, $t_R=7$ min), compound **6** (91.2 mg, $t_R=15$ min), eleutherinoside D (**3**, 4.5 mg, $t_R=18$ min), eleutherinoside B (**1**, 26.2 mg, $t_R=20$ min), eleutherinoside C (**2**, 33.7 mg, $t_R=23$ min) and compound **7** (104.8 mg, $t_R=33$ min). The EtOAc layer was then separated on a silica gel PSQ100B column ($\phi=27\times490$ mm) to give fraction 5b (219 mg, eluted with 2000 mL of Hexane/EtOAc 8.5:1.5, 10.4% inhibition at 2.5 μg mL^{-1}), 5c, and 5d (458 and 133 mg, eluted with 200 mL of hexane/EtOAc 7.5:2.5 , 94.7% inhibition at 2.5 μg mL^{-1}), 5e, 5f (48 and 44 mg, eluted with 200 mL of hexane/EtOAc 7:3, 99.5% and 74.3% inhibition, respectively), and 5g (compound **11**; 43 mg, eluted with 200 mL of hexane/EtOAc 7:3, 94.6% inhibition), 5 h, 5i, and 5j (155, 357, and 570 mg, eluted with 1100 mL of hexane/EtOAc 5:5, EtOAc/acetone 5:5, and MeOH; 56.1%, 18.4%, and 21.9% inhibition at 2.5 μg mL^{-1}, respectively). Fraction 5c was purified by ODS-HPLC (YMC pack Pro C18 column, $\phi=10\times250$ mm; eluted with 70% aqueous MeOH; flow rate, 2 mL min^{-1}) to give compounds **15**, **13**, and **14** (2.6, 14.4, and 74.0 mg, $t_R=12$, 19 and 22 min, respectively). Fraction 5d was purified by ODS-HPLC (the same column; eluted with 65% aqueous MeOH; flow rate, 2 mL min^{-1}) to give compound **9** (42.4 mg, $t_R=28$ min). Fraction 5e was purified by ODS-HPLC (the same column; eluted with 66% aqueous MeOH; flow rate, 2 mL min^{-1}) to give compound **12** (2.3 mg, $t_R=22$ min). Fraction 5f was purified by ODS-HPLC (the same column; eluted with 65% aqueous MeOH; flow rate, 2 mL min^{-1}) to give compounds **8** and **10** (6.3 and 6.6 mg, $t_R=12$ and 18 min, respectively).

Eleutherinoside B (**1**): Reddish brown powder, FAB-MS *m/z* 615 $[M+H]^+$; HRFABMS *m/z* 615.2336, calcd for $C_{28}H_{39}O_{15}$ $[M+H]^+$, 615.2289; IR (ATR):$\tilde{\nu}_{max}=3326$, 2932, 1611, 1241, 901, and 808 cm^{-1}; UV (MeOH) λ_{max} nm (log ε) 340 (4.7), 326 (4.7), 311 (4.7), and 234 (4.8); $[\alpha]_D^{24}=-2.7$ ($c=1.0$, MeOH/H_2O 1:1); ^1H and ^{13}C NMR data in Table 2.

Eleutherinoside C (**2**): Reddish brown powder, FAB-MS *m/z* 599 $[M+H]^+$, 637 $(M+K)^+$; HRFABMS *m/z* 637.1887, calcd for $C_{28}H_{38}O_{14}K$ $[M+K]^+$, 637.1899; IR (ATR): $\tilde{\nu}_{max}=3365$, 1610, 1361, 1058, 836, and 751 cm^{-1}; UV (MeOH) λ_{max} nm (log ε) 337 (4.0), 324 (4.0), and 236 (4.9); $[\alpha]_D^{24}=-5.0$ ($c=0.25$, MeOH/H_2O 1:1); ^1H and ^{13}C NMR data in Table 2.

Eleutherinoside D (**3**): Reddish brown powder, FAB-MS *m/z* 571 $[M+H]^+$, 609 $[M+K]^+$; HRFABMS *m/z* 609.1575, calcd for $C_{26}H_{34}O_{14}K$ $[M+K]^+$, 609.1586; IR (ATR): $\tilde{\nu}_{max}=3651$, 1659, 1198, and 751 cm^{-1}; UV (MeOH) λ_{max} nm (log ε) 334 (4.6), 319 (4.6), 306 (4.6), and 234 (4.9); $[\alpha]_D^{24}=-10.9$ ($c=0.2$, MeOH/H_2O 3:2); ^1H and ^{13}C NMR data in Table 2.

Eleutherinoside E (**4**): Yellow powder, FAB-MS *m/z* 571 $[M+H]^+$, 609 $[M+K]^+$; HRFABMS *m/z* 609.1566, calcd for $C_{26}H_{34}O_{14}K$ $[M+K]^+$, 609.1586; IR (ATR): $\tilde{\nu}_{max}$3308, 1604, 1198, and 841 cm^{-1}; UV (MeOH) λ_{max} nm (log ε) 366 (3.5), 339 (3.9), and 228 (4.7); $[\alpha]_D^{24}=-26.0$ ($c=0.50$ MeOH/H_2O 1:1); ^1H and ^{13}C NMR data in Table 2.

Enzymatic hydrolysis of eleutherinosides A–E: Eleutherinoside A (**5**, 9.0 mg) in HOAc/NaOAc buffer (pH 4.3, 4.5 mL) was treated with naringinase (45.0 mg, Wako) at 37°C for 23 h. After cooling to room temperature, water was added to the reaction mixture, and the mixture was partitioned with EtOAc. The aglycon in the EtOAc layer was purified by preparative TLC eluted with hexane/EtOAc 2:3. The sugar in the aqueous layer was purified by passage through an ODS sep-pak column. Eleutherinoside B (**1**, 6.4 mg), eleutherinoside C (**2**, 5.7 mg), eleutherinoside D (**3**, 1.0 mg), and eleutherinoside E (**4**, 1.0 mg) were treated in the same way as **1** to yield aglycons and sugars of each compound. The aglycon of **2** (2.1 mg) was found to be identical with isoeleutherin (**9**) by a comparison of NMR and $[\alpha]_D$ data. The aglycon of **3** (0.3 mg) was identical with **12** by a comparison of NMR and $[\alpha]_D$ data with literature data.

Comparison of optical data of **12** and ventilong C: CD (MeOH) for **12**: λ_{max} nm ($\Delta\varepsilon$) 261 (−0.35), 301 (0.42), 393 (−0.12); CD (MeOH) for ventilong C:[13] λ_{max} nm ($\Delta\varepsilon$) 280 (−0.17), 320 (0.09), 408 (−0.15). Optical rotation: **12**, $[\alpha]_D^{24}=+41.5$ ($c=1.00$, $CHCl_3$); ventilong C,[13] $[\alpha]_D^{22}=+144$ ($c=0.16$, $CHCl_3$).

HPLC analysis of sugar components in eleutherinosides B–E: The sugars obtained by hydrolysis of eleutherinosides B–E (0.5 mg of each) were dissolved in pyridine (1 mL) and treated with L-cysteine methyl ester hydrochloride (2 mg) at 60°C for 1 h. The resulting thiazolidine derivatives were analyzed by HPLC. HPLC conditions: detection: UV at 210 nm; column: Inertsil NH_2 ($\phi=4.6\times250$ mm); eluent: 95–75% CH_3CN/H_2O for 60 min, linear gradient; flow rate: 1 mL min^{-1}. Each retention time was identical with that of the authentic sample. Methyl-2-(D-gluco-pentahydroxypentyl)thiazolidine-4(*R*)-carboxylate: $t_R=23.4$ and 29.4 min; methyl-2-(L-glucopentahydroxypentyl)thiazolidine-4(*R*)-carboxylate: $t_R=$ 24.6 and 28.8 min.

Isolation of cellular extracts: SW480 cells (5×10^5) were seeded into 60 mm dishes, and after 24 h of incubation were treated with compound **9** for 24 h. Cells were then collected by scraping and whole cell protein was obtained by lysing the cells in ice-cold lysis buffer containing 20 mM Tris-HCl (pH 7.4), 150 mM NaCl, 1% Triton X-100, 1% Sodium deoxycholate, 0.1% SDS, 0.1 mM NaF, and 1% protease inhibitor cocktail (Nakarai tesque Inc.) for 20 min. The lysates were centrifuged at 13000 rpm, 4°C for 30 min and supernatants were stored at −80°C before use.

Isolation of cytoplasmic and nuclear proteins: SW480 cells were treated in the same way as the cellular extract. Cells were then tripsinized and cytoplasmic and nuclear proteins were obtained using NE-PER nuclear and cytoplasmic extraction reagents (Pierce) following the manufacturer's protocol, and the proteins were stored at −80°C.

Western blot analysis: A Western blot analysis for the presence of β-catenin, Tcf-4, and c-myc was performed with the whole extract, cytosol, or nuclear proteins from SW480. Proteins were isolated as described above. Protein was mixed 4:1 with 5× sample buffer (20% 2-ME, 20% sucrose, 8% SDS, 0.02% bromophenol blue, and 0.4 M Tris-HCl, pH 6.8), loaded onto a 10% SDS-PAGE gel, and run at 20 mA for 2 h. Proteins were transferred electrophoretically onto a Immun-blot PVDF membrane (Bio-Rad). After blocking with 5% milk in TBST, the membrane was incubated at room temperature with the primary Ab (anti-β-catenin, BD Biosciences; c-myc, and Tcf-4 antibody, Santa Cruz Biotechnology, Santa Cruz, CA; or anti-β-actin, Sigma) for 1 h. β-Actin was used as an internal control. After being washed with TBST, the membrane was incubated at room temperature with HRP-conjugated anti-IgG AB (Sigma). After further washing with TBST, immunoreactive bands were detected using the Immobilon Western chemiluminescent HRP substrate (Millipore).

General experimental procedures: FAB-MS was measured on a JEOL JMS-AX500 spectrometer, and high-resolution FABMS spectra were obtained on a JEOL JMS-HX110 spectrometer. NMR spectra were recorded on JEOL JNM GSX-A400, A500, and ecp600 spectrometers with a deuterated solvent whose chemical shift was taken as an internal standard. IR spectra were measured on ATR in a JASCO FT-IR 230 spectrophotometer. UV spectra were measured in a Shimadzu UV mini-1240 spectrometer. Optical rotations were measured with a JASCO P-1020 polarimeter, and CD spectra were obtained on a JASCO J-720WI spectropolarimeter.

Acknowledgements

We thank Prof. Jeremy Nathans (Johns Hopkins Medical School) for kindly offering the STF/293 cells and Prof. Randall T. Moon (University of Washington) for the SuperTopflash and SuperFopflash reporter plasmids. We thank Dr. Masaaki Sato for helpful discussions in the beginning of this study. This work was partly supported by a Grant-in-Aid from the Ministry of Education, Culture, Sports, Science, and Technology of Japan.

[1] R. H. Giles, J. H. van Es, H. Clevers, *Biochim. Biophys. Acta Rev. Cancer* **2003**, *1653*, 1–24.
[2] C. Y. Logan, R. Nusse, *Annu. Rev. Cell Dev. Biol.* **2004**, *20*, 781–810.
[3] Q. Xu, Y. Wang, A. Dabdoub, P. M. Smallwood, J. Williams, C. Woods, M. W. Kelley, L. Jiang, W. Tasman, K. Zhang, J. Nathans, *Cell* **2004**, *116*, 883–895.
[4] C. M. Hedgepeth, L. J. Conrad, J. Zhang, H. C. Huang, V. M. Lee, P. S. Klein, *Dev. Biol.* **1997**, *185*, 82–91.
[5] V. Stambolic, L. Ruel, J. R. Woodgett, *Curr. Biol.* **1996**, *6*, 1664–1668.
[6] a) S. Paramapojn, M. Ganzera, W. Gritsanapan, H. Stuppner, *J. Pharm. Biomed. Anal.* **2008**, *47*, 990–993; b) H. Shibuya, T. Fukushima, K. Ohashi, A. Nakamura, S. Riswan, I. Kitagawa, *Chem. Pharm. Bull.* **1997**, *45*, 1130–1134.
[7] M. Piggott, D. Wege, *Aust. J. Chem.* **2003**, *56*, 691–702.
[8] Z. Chen, H. Huang, C. Wang, Y. Li, J. Ding, U. Sankawa, H. Noguchi, Y. Iitaka, *Chem. Pharm. Bull.* **1986**, *34*, 2743–2746.
[9] S. Kitanaka, M. Takahashi, M. Takido, *Phytochemistry* **1990**, *29*, 350–351.
[10] J. Xu, F. Qiu, G. Qu, N. Wang, X. Yao, *Zhongguo Yaowu Huaxue Zazhi* **2005**, *15*, 157–161.
[11] T. M. A. Alves, H. Kloos, C. L. Zani, *Mem. Inst. Oswaldo Cruz* **2003**, *98*, 709–712.
[12] S. Hara, H. Okabe, K. Mihashi, *Chem. Pharm. Bull.* **1987**, *35*, 501–506.
[13] T. Hanumaiah, G. S. R. Rao, C. P. Rao, K. V. J. Rao, *Tetrahedron* **1985**, *41*, 635–642.
[14] C. H. Park, J. Y. Chang, E. R. Hahm, S. Park, H. K. Kim, C. H. Yang, *Biochem. Biophys. Res. Commun.* **2005**, *328*, 227–234.
[15] W. Hodge, D. Taylor, *Webbia* **1956**, *12*, 513–644.
[16] M. E. van den Berg "Ver-o-peso: the ethnobotany of an Amazonian market" in *Advances in Economic Botany*, (Eds: G. T. Prance, J. A. Kallunki), Bronx, New York, **1984**.
[17] J. Lin, T. Puckree, T. Mvelase, *J. Ethnopharmacol.* **2002**, *79*, 53–56.
[18] B. Weniger, M. Haag-Berrurier, R. Anton, *J. Ethnopharmacol.* **1982**, *6*, 67–84.
[19] J. Ding, H. Huang, *Zhongcaoyao* **1983**, *14*, 351–352.
[20] H. Hara, N. Maruyama, S. Yamashita, Y. Hayashi, K. Lee, K. Bastow, R. Marumoto, Y. Imakura, *Chem. Pharm. Bull.* **1997**, *45*, 1714–1716.
[21] E. B. Thompson, *Annu. Rev. Physiol.* **1998**, *60*, 575–600.
[22] S. Dihlmann, von Knebel M. Doeberitz, *Int. J. Cancer* **2005**, *113*, 515–524.
[23] R. Larsson, J. Kristensen, C. Sandberg, P. Nygren, *Int. J. Cancer* **1992**, *50*, 177–185.
[24] K. Kaniwa, M. A. Arai, X. Li, M. Ishibashi, *Bioorg. Med. Chem. Lett.* **2007**, *17*, 4254–4257.
[25] S. Hanazawa, M. A. Arai, X. Li, M. Ishibashi, *Bioorg. Med. Chem. Lett.* **2008**, *18*, 95–98.

Received: September 11, 2008
Published online: December 8, 2008

